



Long wavelength perfect fluidity from short distance jet transport in quark-gluon plasmas

Jiechen Xu^a, Jinfeng Liao^{b,c}, Miklos Gyulassy^a

^aDepartment of Physics, Columbia University, 538 West 120th Street, New York, NY, USA

^bPhysics Department and CEEM, Indiana University, 2401 North Milo B. Sampson Lane, Bloomington, IN 47408, USA

^cRIKEN BNL Research Center, Building 510A, Brookhaven National Laboratory, Upton, NY 11973, USA

Abstract

We build a new phenomenological framework that bridges the long wavelength bulk viscous transport properties of the strongly-coupled quark-gluon plasma (sQGP) and short distance hard jet transport properties in the QGP. The full nonperturbative chromo-electric (E) and chromo-magnetic (M) structure of the near “perfect fluid” like sQGP in the critical transition region are integrated into a semi-Quark-Gluon-Monopole Plasma (sQGMP) model lattice-compatibly and implemented into the new CUJET3.0 jet quenching framework. All observables computed from CUJET3.0 are found to be consistent with available data at RHIC and LHC simultaneously. A quantitative connection between the shear viscosity and jet transport parameter is rigorously established within this framework. We deduce the $T = 160–600$ MeV dependence of the QGP’s η/s : its near vanishing value in the near T_c regime is determined by the composition of E and M charges, it increases as T rises, and its high T limit is fixed by color screening scales.

Keywords: Relativistic Heavy Ion Collisions, Jet Quenching, Perfect Fluidity, Quark-Gluon Plasmas

1. Introduction

To probe the fundamental properties of hot quark matter and the mechanism of color confinement through ultrarelativistic nucleus-nucleus collisions, it is necessary to consider both the perturbative and nonperturbative aspects of QCD carefully in heavy-ion phenomenology. Present quantitative analyses of the strongly-coupled quark-gluon plasma (sQGP) created in A+A reactions at RHIC and LHC [1] nevertheless divide in the two aspects: on the one hand, in the “soft” nonperturbative regime, the low transverse momentum (p_T) long wavelength “perfect fluidity” of the sQGP is described by relativistic hydrodynamical simulations; on the other hand, in the “hard” regime, high p_T short distance jet transport properties in the QGP computed from perturbative QCD (pQCD) models are compatible with a wide range of data [2]. A unified framework incorporating both aspects is however missing; it is therefore challenging to translate conveniently between heavy-ion and confinement physics.

Concentrated on pQCD, to build up such a framework, both the long and short distance transport properties of the QGP must be accounted for more systematically. In the “soft” sector, the “perfect fluid” like sQGP has a near vanishing shear viscosity to entropy density ratio $\eta/s = 1/4\pi$ bounded by quantum fluctuations [3, 4], however from leading order (LO) pQCD estimate, the QGP in the weakly-coupled limit (wQGP) has an $\eta/s \approx 0.071(\alpha_s^2 \log(1/\alpha_s))^{-1}$ that approaches 1 [5]. In the “hard” sector, it has been found

that most jet energy loss models can describe the high p_T light hadrons' and open heavy flavors' nuclear modification factor (R_{AA}) data, but the azimuthal elliptic anisotropy (v_2) is underestimated by 50% at RHIC and LHC near-universally [8].

The above necessitates (1) exploring the full nonperturbative chromo-electric (E) and chromo-magnetic (M) structure of QCD in the region near the critical transition temperature (T_c), (2) developing a microscopic, lattice-compatible description of the sQGP, and (3) implementing it into a systematic pQCD jet energy loss model and testing with high p_T data. The new CUJET3.0 framework achieved all of them [9].

2. The CUJET3.0 framework

In CUJET3.0 [9], accounting for both chromo-electric (E) and chromo-magnetic (M) quasi-particles (QPs) as in the EM seesaw scenario proposed by Liao and Shuryak [10], the dynamical running coupling DGLV [11] energy loss kernel in CUJET2.0 [12] is generalized to:

$$x \frac{dN}{dx} \propto \int d^2q \left[\frac{\rho \alpha_s^2(\mathbf{q}_\perp^2) f_E^2}{\mathbf{q}_\perp^2 (\mathbf{q}_\perp^2 + f_E^2 \mu^2)} \right] \dots \rightarrow \int d^2q \left[\frac{\rho_E (\alpha_s(\mathbf{q}_\perp^2) \alpha_s(\mathbf{q}_\perp^2)) f_E^2}{\mathbf{q}_\perp^2 (\mathbf{q}_\perp^2 + f_E^2 \mu^2)} + \frac{\rho_M (\alpha_E(\mathbf{q}_\perp^2) \alpha_M(\mathbf{q}_\perp^2)) f_M^2}{\mathbf{q}_\perp^2 (\mathbf{q}_\perp^2 + f_M^2 \mu^2)} \right] \dots \quad (1)$$

Here $\alpha_s(Q^2) \equiv \alpha_E(Q^2) = \alpha_c/[1 + \frac{9\alpha_c}{4\pi} \log(\frac{Q^2}{T_c^2}) \cdot 1_{Q>T_c}]$, $T_c = 160$ MeV, and $\alpha_E \cdot \alpha_M = 1$ for any Q^2 because of Dirac quantization [10]. The total quasi-particle number density ρ consists of EQPs with fraction $\chi_T = \rho_E/\rho$ and MQPs with fraction $1 - \chi_T = \rho_M/\rho$. The color electric charges are suppressed near T_c as in the semi-QGP model [13], $\chi_T \equiv \chi_T^L = c_q L + c_g L^2$, where the Polyakov loop $L(T) \propto \langle \text{tr} \mathcal{P} \exp(i g \int_0^{1/T} A_0 d\tau) \rangle$ is renormalized such that $L(T \rightarrow \infty) = 1$, c_q and c_g are Stefan-Boltzmann fraction coefficients. In the critical transition region, the semi-QGP degrees of freedom (DOFs) and emergent chromo-magnetic monopoles form a semi-Quark-Gluon-Monopole Plasma (sQGMP) [9, 14]. The parameter f_E and f_M is defined via $f_E \equiv \mu_E/\mu = \sqrt{\chi_T}$ and $f_M \equiv \mu_M/\mu = c_m g$, where μ_E and μ_M is the E and M screening mass respectively, and $g = \sqrt{4\pi\alpha_s(\mu^2)} = \mu/(T \sqrt{1 + N_f/6})$.

The $L(T)$, $\mu_{E,M}(T)$, $\rho/T^3 \sim p/T^4 = \frac{1}{VT^3} \log Z$, and equation of state (EOS) are all constrained by lattice QCD data, as shown in Fig. 1. A theoretical uncertainty in CUJET3.0 is originated from choosing the diagonal u-quark number susceptibility $\chi_2^u(T) = \frac{\partial^2(p/T^4)}{\partial(\mu_u/T)^2} = \frac{1}{VT^3} \langle N_u^2 \rangle$ over the Polyakov loop for the quark deconfinement rate, i.e. $\chi_T \rightarrow \chi_T^u = c_q \chi_2^u(T)/\chi_2^u(\infty) + c_g L^2$, which will be analyzed lately. All other computational details in CUJET3.0 are the same as in CUJET2.0, including the 2+1D viscous hydrodynamical background profiles generated from VISHNU simulations [15].

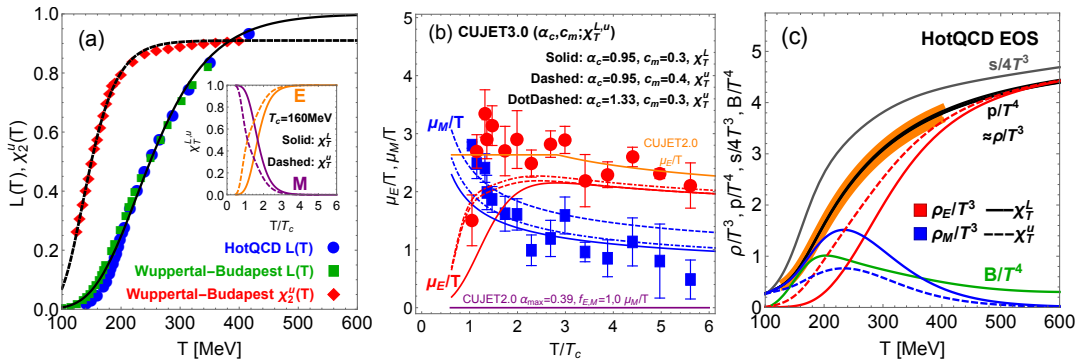


Fig. 1. (Color online) (a) The parameterized fit to lattice QCD data [6] of the renormalized Polyakov loop L and diagonal light quark susceptibility χ_2^u in the χ_T^L and χ_T^u scheme within CUJET3.0. The inset shows the chromo-electric (E) and chromo-magnetic (M) quasi-particle fractions in corresponding schemes. (b) The temperature dependence of the E and M screening mass $\mu_{E,M}$ in CUJET2.0 (HTL QGP) and CUJET3.0 (sQGMP) compare with lattice simulations [7]. (c) The HotQCD equation of state (EOS), pressure p , entropy density s [6], the “bag” pressure (B), as well as the E and M quanta number density $\rho_{E,M}$ embedded in the CUJET3.0 framework.

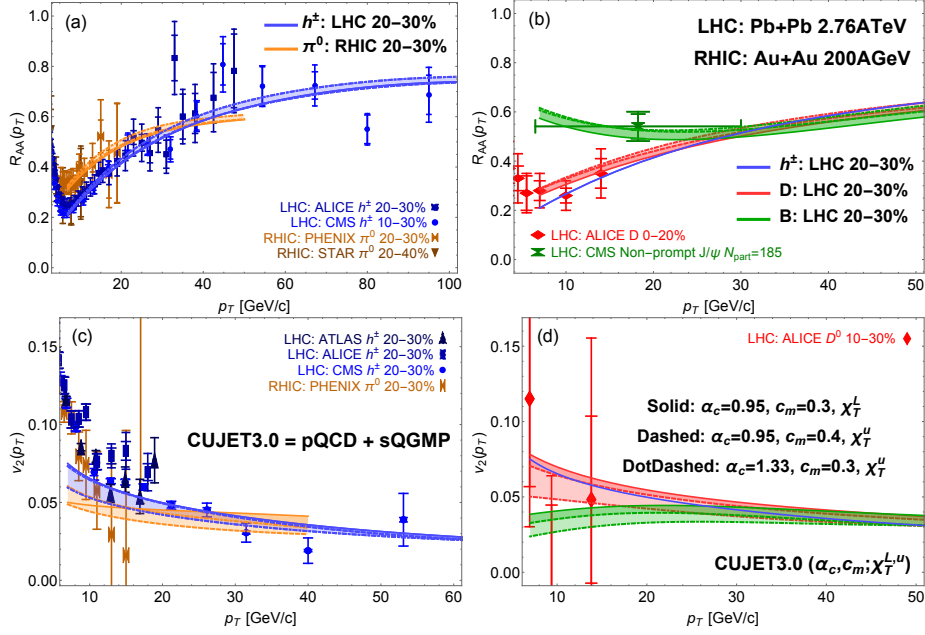


Fig. 2. (Color online) CUJET3.0 results of (a) light hadron (LH, neutral pion π^0 and charge particle h^\pm)’s R_{AA} , (b) open heavy flavor (HF, B meson and prompt D meson)’s R_{AA} , (c) LH’s v_2 , and (d) HF’s v_2 , at high $p_T > 8\text{GeV}$ in semi-peripheral A+A collisions, compared with data from RHIC and LHC [2]. The variations of predicted jet quenching observables from different schemes within CUJET3.0 suggest that data on high p_T leading hadron R_{AA} and v_2 in heavy-ion collisions can rigorously constrain the nonperturbative chromo-electric and chromo-magnetic structure of the QCD matter near T_c , and provide critical information about color confinement.

3. Results and discussions

Jet quenching observables from three different schemes in the CUJET3.0 framework will be studied: (i) $\alpha_c=0.95$, $c_m=0.3$, χ_T^L ; (ii) $\alpha_c=0.95$, $c_m=0.4$, χ_T^u ; (iii) $\alpha_c=1.33$, $c_m=0.3$, χ_T^u . The parameter set (α_c, c_m) is constrained by the reference datum at LHC 20–30% Pb+Pb $\sqrt{s_{NN}} = 2.76\text{TeV}$ $R_{AA}^{h^\pm}(p_T = 12.5\text{GeV}) \approx 0.3$ and lattice date of $\mu_{E,M}(T)$ as shown in Fig. 1(b). Fig. 2 compares the CUJET3.0 results of leading light hadron (LH) and open heavy flavor (HF)’s $R_{AA}(p_T > 8\text{GeV})$ and $v_2(p_T > 8\text{GeV})$ at RHIC and LHC semi-peripheral A+A collisions with corresponding data.

For high p_T LHs, all three schemes can simultaneously describe the R_{AA} and v_2 data at RHIC and LHC. The phenomenon that scheme (i) and (ii) generate a relatively larger v_2 than scheme (iii) implies that the azimuthal asymmetry is sensitive to how the relative value of μ_E and μ_M inverses near T_c – the higher the inversion temperature, the longer the path length that jets interact with the monopole dominated medium at later time of the QGP evolution, the larger the high p_T v_2 .

For open heavy flavors, scheme (ii) and (iii)’s R_{AA} overlap, both are larger than scheme (i)’s. Since the former two have the same color deconfinement scheme χ_T^u that is different from the latter’s χ_T^L , it is implicit that the HF’s high p_T R_{AA} in CUJET3.0 is sensitive to the rate at which electric DOFs are liberated ($r_d = d\chi_T/dT$), i.e. the detailed composition of E and M DOFs near T_c . Meanwhile, Fig. 2(d) shows that the HF’s v_2 ’s are all different in scheme (i)(ii)(iii). It is therefore fair to conclude that the open charm and beauty’s $R_{AA}(p_T)$ and $v_2(p_T)$ are excellent probes of the nonperturbative E and M structure of the sQGMP (r_d, μ_E, μ_M) near T_c within CUJET3.0.

The jet transport parameter $\hat{q}(T, E) \equiv \langle q_\perp^2 \rangle / \lambda$ in CUJET3.0 and CUJET2.0 can be extracted as in [9] and [12, 17] respectively. They are plotted in Fig. 3(a). Extrapolated $\hat{q}(T, E)$ down to thermal energy scales $E \sim 3T$, one can estimate the η/s using kinetic theory, i.e. $\eta/s = \frac{1}{s} \frac{4}{15} \sum_a \rho_a \langle p \rangle_a \lambda_a^\perp = \frac{18T^3}{5s} \sum_a \rho_a / \hat{q}_a(T, E = 3T)$, where $\rho_a(T)$ is the quasi-parton number density of type $a = q, g, m$. The η/s results from both CUJET3.0 and CUJET2.0 are shown in Fig. 3(b).

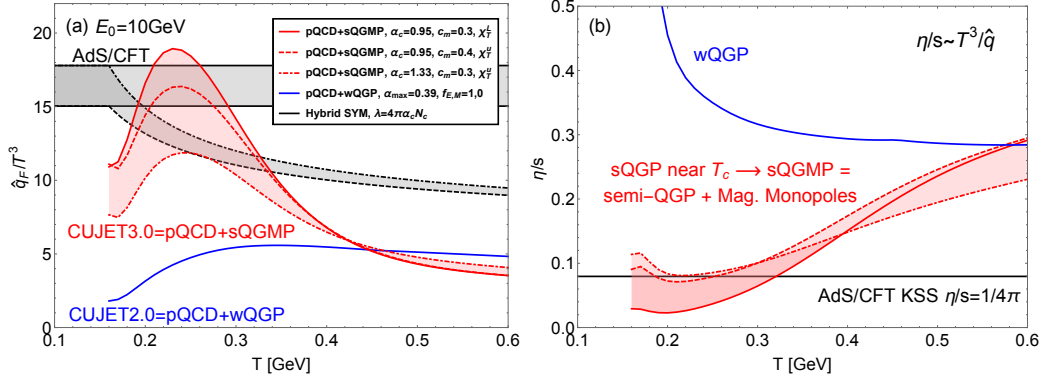


Fig. 3. (Color online) (a) The temperature dependence of the scaled jet transport parameter \hat{q}_F/T^3 for a quark jet (in the fundamental representation F of $SU(N_c=3)$) with initial energy $E_0 = 10$ GeV in various schemes within the CUJET3.0 framework, compared with the CUJET2.0 counterpart, as well as $N = 4$ Supersymmetric Yang-Mills (SYM) \hat{q}_{SYM} results from leading order (LO) AdS/CFT calculations ($\hat{q}_{SYM} = [\pi^{3/2}\Gamma(3/4)/\Gamma(5/4)] \sqrt{\lambda} T_{SYM}^3$) [16]. Note that $3T_{SYM}^3 \approx T^3$ because of different number of degrees of freedom in $N_c = 3$ SYM and three-flavor QCD [17]. The gray band with dashed black edges corresponds to using 't Hooft coupling $\lambda = 12\pi\alpha_s(Q^2)$. (b) The shear viscosity to entropy density ratio η/s estimated in the kinetic theory extrapolation $\eta/s \sim T^3/\hat{q}$ from jet quenching parameters in panel (a). Note that $T_c = 160$ MeV. In CUJET3.0, a clear \hat{q}_F/T^3 maximum and η/s minimum appear at $T \sim 1.3 - 1.4T_c$ where the scaled number density of emergent chromo-magnetic monopoles near T_c peaks. The $(\eta/s)_{min}$ is influenced by fractions of E and M composites, hence is sensitive to confinement physics. Its value in both $\chi_T^{L,u}$ schemes converge to approximately the KSS quantum bound $\eta/s = 1/4\pi$ [4]. At high T , the η/s from sQGMP and weakly-coupled QGP (wQGP) coincide because of similar color screening structures.

At high T where MQPs vanish as $\chi_T \rightarrow 1$, the η/s of sQGMP and weakly-coupled QGP (wQGP) overlap because of similar $\mu_E(T)$'s. In CUJET3.0, through fixing $\eta/s \sim T^3/\hat{q}$ at all temperatures, as T cools down, η/s drops, and a shear viscosity minimum appears at $T \sim 1.3 - 1.4T_c$, coinciding with the temperature where ρ_M/T^3 peaks as shown in Fig. 1(c). The value of $(\eta/s)_{min}$ is determined by the deconfinement scheme $\chi_T^{L,u}$, i.e. EQP and MQP fractions near T_c , and it approaches the KSS quantum bound $\eta/s = 1/4\pi$ [4]. These indicate within the CUJET3.0 framework, the long wavelength “perfect fluidity” of the sQGP is generated from short distance jet transport properties controlled by \hat{q} , and a quantitative $\eta/s \sim T^3/\hat{q}$ connection is robustly established in a wide temperature range.

4. Summary

We conclude that taking full advantage of the new CUJET3.0 jet energy loss framework, data of high p_T light hadron (LH) and open heavy flavor (HF)'s R_{AA} and v_2 in heavy-ion collisions at RHIC and LHC can provide stringent constraints on the nonperturbative properties of the QCD matter near T_c . After fixed model parameters with LH's R_{AA} data, (1) LH's v_2 regulates the E and M screening mass difference ($\mu_E(T) - \mu_M(T)$) near T_c , (2) HF's R_{AA} determines the rate at which color DOFs are deconfined ($r_d(T)$), (3) HF's v_2 distinguishes $r_d(T)$, $\mu_E(T)$ and $\mu_M(T)$.

In the CUJET3.0 framework, after included the semi-QGP suppression of chromo-electric charges and the emergence of chromo-magnetic monopoles in the nonperturbative near-critical QGP, the long wavelength “perfect fluidity” ($\eta/s \sim 1/4\pi$) is successfully generated from the short distance hard parton transport properties that are controlled by the jet quenching parameter \hat{q} . Within this framework, a robust $\eta/s \sim T^3/\hat{q}$ connection is established in all temperature ranges above T_c . Overall, CUJET3.0 provides a quantitative bridge between heavy-ion phenomenology and fundamental confinement physics.

We thank Peter Petreczky for insightful discussions. JX acknowledges helpful conversations with Gabriel Denicol, Rob Pisarski, Chun Shen and Xin-Nian Wang. The research of JX and MG is supported by U.S. DOE Nuclear Science Grants No. DE-FG02-93ER40764. The research of JL is supported by the National Science Foundation (Grant No. PHY-1352368). JL also acknowledges partial support from the RIKEN BNL Research Center.

References

- [1] M. Gyulassy and L. McLerran, Nucl. Phys. A **750**, 30 (2005).
- [2] B. Abelev *et al.* [ALICE Collaboration], Phys. Lett. B **719**, 18 (2013); Phys. Lett. B **720**, 52 (2013); G. Aad *et al.* [ATLAS Collaboration], Phys. Lett. B **707**, 330 (2012); S. Chatrchyan *et al.* [CMS Collaboration], Eur. Phys. J. C **72**, 1945 (2012); Phys. Rev. Lett. **109**, 022301 (2012); A. Adare *et al.* [PHENIX Collaboration], Phys. Rev. Lett. **101**, 232301 (2008); **105**, 142301 (2010); Phys. Rev. C **87**, 034911 (2013); B. I. Abelev *et al.* [STAR Collaboration], Phys. Rev. C **80**, 044905 (2009).
- [3] P. Danielewicz and M. Gyulassy, Phys. Rev. D **31**, 53 (1985).
- [4] P. Kovtun, D. T. Son and A. O. Starinets, Phys. Rev. Lett. **94**, 111601 (2005).
- [5] T. Hirano and M. Gyulassy, Nucl. Phys. A **769**, 71 (2006).
- [6] A. Bazavov *et al.*, Phys. Rev. D **80**, 014504 (2009); S. Borsanyi *et al.* [Wuppertal-Budapest Collaboration], JHEP **1009**, 073 (2010); S. Borsanyi, Z. Fodor, S. D. Katz, S. Krieg, C. Ratti and K. Szabo, JHEP **1201**, 138 (2012).
- [7] A. Nakamura, T. Saito and S. Sakai, Phys. Rev. D **69**, 014506 (2004).
- [8] B. B. Abelev *et al.* [ALICE Collaboration], Phys. Rev. C **90**, no. 3, 034904 (2014); S. Cao, G. Y. Qin and S. A. Bass, Phys. Rev. C **92**, 024907 (2015); B. Betz and M. Gyulassy, JHEP **1408**, 090 (2014) [JHEP **1410**, 043 (2014)]; arXiv:1503.07671 [hep-ph]; D. Molnar and D. Sun, arXiv:1305.1046 [nucl-th].
- [9] J. Xu, J. Liao and M. Gyulassy, Chin. Phys. Lett. **32**, 092501 (2015); arXiv:1508.00552 [hep-ph].
- [10] J. Liao and E. Shuryak, Phys. Rev. C **75**, 054907 (2007); Phys. Rev. Lett. **101**, 162302 (2008); **102**, 202302 (2009).
- [11] M. Gyulassy *et al.*, Nucl. Phys. B **594**, 371 (2001); M. Djordjevic *et al.*, Nucl. Phys. A **733**, 265 (2004); Phys. Rev. Lett. **101**, 022302 (2008); S. Wicks *et al.*, Nucl. Phys. A **784**, 426 (2007); A. Buzzatti *et al.*, Phys. Rev. Lett. **108**, 022301 (2012).
- [12] J. Xu, A. Buzzatti and M. Gyulassy, JHEP **1408**, 063 (2014); Nucl. Phys. A **932**, 128 (2014).
- [13] R. D. Pisarski, Phys. Rev. D **74**, 121703 (2006); Y. Hidaka and R. D. Pisarski, Phys. Rev. D **78**, 071501 (2008); **81**, 076002 (2010); A. Dumitru *et al.*, **86**, 105017 (2012); C. Gale *et al.*, Phys. Rev. Lett. **114**, 072301 (2015).
- [14] B. G. Zakharov, JETP Lett. **101**, 587 (2015); A. Iwazaki, arXiv:1511.02271 [hep-ph].
- [15] H. Song and U. W. Heinz, Phys. Rev. C **78**, 024902 (2008); C. Shen, U. Heinz, P. Huovinen and H. Song, Phys. Rev. C **82**, 054904 (2010); C. Shen, Z. Qiu, H. Song, J. Bernhard, S. Bass and U. Heinz, Comput. Phys. Commun. **199**, 61 (2016).
- [16] H. Liu, K. Rajagopal and U. A. Wiedemann, Phys. Rev. Lett. **97**, 182301 (2006).
- [17] K. M. Burke *et al.* [JET Collaboration], Phys. Rev. C **90**, 014909 (2014).